OCSC00799
A0005

SEISMIC REFLECTION METHODS FOR STUDY OF THE WATER COLUMN

I. Fer, University of Bergen, Bergen, Norway
W. S. Holbrook, University of Wyoming, Laramie, WY, USA

S0005

Introduction

P0005 Recent work has shown that marine seismic reflection profiling, a technique commonly used by geophysicists and geologists to image the Earth's crust beneath the seafloor, can produce surprisingly detailed images of thermohaline fine structure in the ocean. Seismic reflection profiling produces images by mapping the locations of 'bounce points' where acoustic waves expanding out from the shot location have reflected from subsurface interfaces where changes in material density and/or sound speed occur. Similar to sonar, the arrival time of a reflection at a receiver, together with a measurement or estimate of the sound-speed profile, is used to estimate the depth of the feature that generated the reflection.

P0010 Within the ocean, density-compensating, fine-scale (1–10 m thick) temperature-salinity contrasts (e.g., temperature and salinity having opposing contributions to the density to keep the density constant) result in small changes in sound speed that produce weak, but distinct, reflections. Recent studies image returns that are specular reflections from laterally continuous steps or sheets in the ocean's temperature-depth structure. The reflectors imaged in the ocean are 100–1000 times weaker than those from the solid Earth below. However, by increasing the gain of the processing system, oceanic fine structure can be made visible. Until recently, seismologists have been largely unaware of these weak reflections in their data and have not routinely processed returns from the water column, since their focus is on the structure of the Earth. The discovery of seismic reflections from the water column and the ability to image large volumes of the ocean at full depth and at high lateral resolution opens up new possibilities for probing the structure of the ocean with 'seismic oceanography'. Spectacular images of thermohaline fine structure in the ocean have been produced from features such as intrusions, internal waves, and mesoscale eddies.

S0010

Primer on the Method

P0015 Marine seismic reflection data are acquired by firing, at constant distance intervals, a sound source of relatively low-frequency (10–150 Hz) energy produced by an array of air guns towed several meters beneath the sea surface. The data are recorded on hydrophone cables, or streamers, which are typically several kilometers long, contain 40–100 hydrophone channels per kilometer, and are towed 3–8 m below the sea surface. The pressure variations of the reflected sound signals are recorded by hydrophones installed at regular intervals (usually 12.5 m) along the streamer. For a flat reflector, the point in the ocean's interior at which a reflecting ray reaches its maximum depth before reflecting (the 'bottoming' or 'reflecting' point) occurs halfway between the source and the receiver. Therefore, the subsurface sampling interval is half the hydrophone spacing (i.e., usually 6.25 m).

P0020 Reflections appear on the resulting records as curved arrivals whose travel time increases hyperbolically with distance from the source point. With the exception of the direct arrival, refractions are not returned to the streamer from within the water column – only reflections. Shots are fired at intervals of 50–150 m, creating a large volume of overlapping reflections on successive shot records. The vessel maintains a constant speed along a straight track allowing for redundant sampling of a fixed point. Traces on the shot records are re-sorted into common midpoint (CMP) records, which gather together all traces that have a common source–receiver midpoint. The hyperbolic curvature of the reflections in each CMP ensemble is then removed, and the resulting flattened reflections are summed (or stacked) together to create a single trace at each CMP. Summed traces for each CMP are then joined into a stacked section. Each trace in the stack can be thought of as the response that would be generated by a simple, single-channel geometry, that is, the wave field from a single shot that travels downward, reflects off a boundary at normal incidence, and is returned and recorded on a single hydrophone located at the source point. The final processing step is migration, which accounts for any distortions in the stacked section caused by the presence of dipping (nonhorizontal) reflectors. The resulting migrated image resembles a snapshot cross-section of the

acoustic impedance of the ocean and underlying Earth at comparable horizontal and vertical sampling of about 5–10 m.

S0015 ## Comparison with Other Marine Acoustic Technology

P0025 Seismic reflection profiling differs substantially from, and thus complements, the high-frequency acoustic imaging commonly used in oceanography. High-frequency (typically above 10 kHz) ocean acoustics image scatterers in the water column – that is, diffracting bodies with spatial dimensions on the order of the dominant wavelength of the sound source, such as zooplankton, bubble clouds or microstructure of temperature, salinity, or velocity. Scattering theories have been developed to quantify relationship between microstructure intensity or zooplankton concentration to the backscatter strength. Many observational programs have imaged internal waves in shallow water, often two-layer flows in straits that show dramatic patterns of wave growth and breaking, however, high-frequency techniques are limited to ranges of a few hundred meters. For the low-frequency sound (10–150 Hz) of the seismic profiles, scattering theory is inappropriate, because the wavelength of the sound is much larger than the length scale of common scatterers in the ocean.

P0030 Unlike the long-range refracted sound typically used in acoustic tomography in the ocean, the reflections imaged with seismic reflection methods are sensitive to the vertical derivative of the sound speed, rather than the value of the sound speed itself. The travel times of the reflections are sensitive to the average sound speed, but the reflection amplitudes

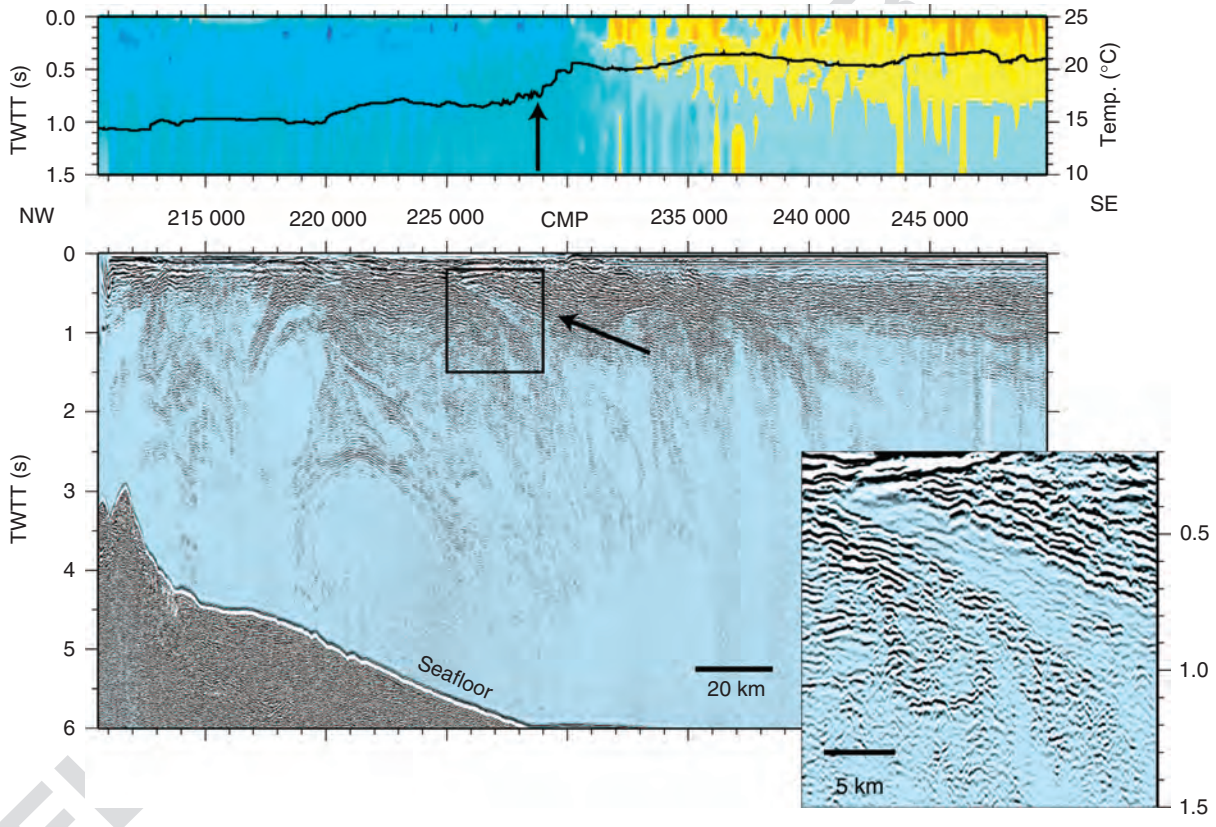

F0005 **Figure 1** (top) Stacking sound speed, approximately equal to root-mean-square sound speed, in the ocean (color) and sea surface temperature (SST, black) measured during a seismic survey in the Newfoundland Basin. Cold colors correspond to low sound speed (minimum of $\sim$1440 m s^{-1}); warm colors reflect higher sound speed (maximum of $\sim$1530 m s^{-1}). Horizontal axis is the common-midpoint (CMP) with 6.25 m spacing. The arrow marks the front between the Labrador current (NW of the front) and the North Atlantic current (SE of the front), visible as an abrupt $\sim$5 °C increase in temperature at CMP 229 000. (bottom) Stacked seismic section of water column with a vertical exaggeration of 27. Vertical axis is two-way-travel time (TWTT) in seconds; the base of the section at 6 s corresponds to a depth of $\sim$4500 m in the ocean. An intrusive feature is marked by an arrow. Box denotes the portion of the profile depicted in the inset which shows slabs losing coherency at depths of $\sim$1000 m. From Holbrook WS, Páramo P, Pearse S, and Schmitt RW (2003) Thermohaline fine structure in an oceanographic front from seismic reflection profiling. *Science* 301: 821–824. Reprinted with permission from AAAS.

are sensitive to the vertical gradients. The frequencies generated by air gun sources are typically in the 10–150 Hz range, corresponding to vertical wavelengths of 10–150 m. The marine seismic reflection method can resolve layers with thickness of about one quarter wavelength, that is, from several meters to several tens of meter thick, provided that the layers are separated by relatively sharp vertical gradients in sound speed as a result of predominantly temperature contrasts. For example, at surface pressure, the sound speed increases by $4\,m\,s^{-1}$ by increasing the temperature of seawater of 35 psu salinity from 5 to 6 °C. The oceanic fine structure is characterized by vertical scales of meters to tens of meters which are not directly affected by molecular diffusion. These scales are comparable to the dominant wavelength of the sound source. Hence, marine seismic reflection data is ideally tuned to detect oceanic fine structure and seismic theory developed for reflections from a laterally coherent layered medium can be confidently applied.

S0020 ## Observations

P0035 To date, published observations using seismic oceanography come from three areas: the North Atlantic Front, the Kuroshio Front, and the Norwegian Sea.

P0040 Seismic reflection data acquired in August 2000 across the oceanographic front between the Labrador current (LC) and the North Atlantic current (NAC) in Newfoundland basin yielded images showing the two-dimensional thermohaline structure of the ocean in unprecedented detail (**Figure 1**). LC and NAC are characterized by cold-fresh and warm-salty water masses, respectively, separated by a front (marked by an arrow in the upper panel of **Figure 1**, LC is on the NW side of the front) where strong thermohaline intrusions with 20- to 30-m-thick fine structure were previously reported. Wedges of inclined reflections in the vicinity of the front are representative of this phenomenon. A plausible mechanism that creates intrusive layers is double diffusion driven solely by the factor 100 difference between the molecular diffusivity of heat and salt. Temperature-salinity structure in the intrusive layers is modified by the fluxes induced by double diffusion when both salinity and temperature increase or decrease with depth. The strong tilt of the reflections matches the expected inclination of density surfaces affected by double-diffusive processes. Nearly horizontal, 0.5- to 5-km-long reflections in the warm waters of the NAC are consistent with the weak tilt of lateral intrusions as a result of double-diffusive mixing observed previously in the NAC, whereas the isopycnal surfaces tilt more strongly in the vicinity of

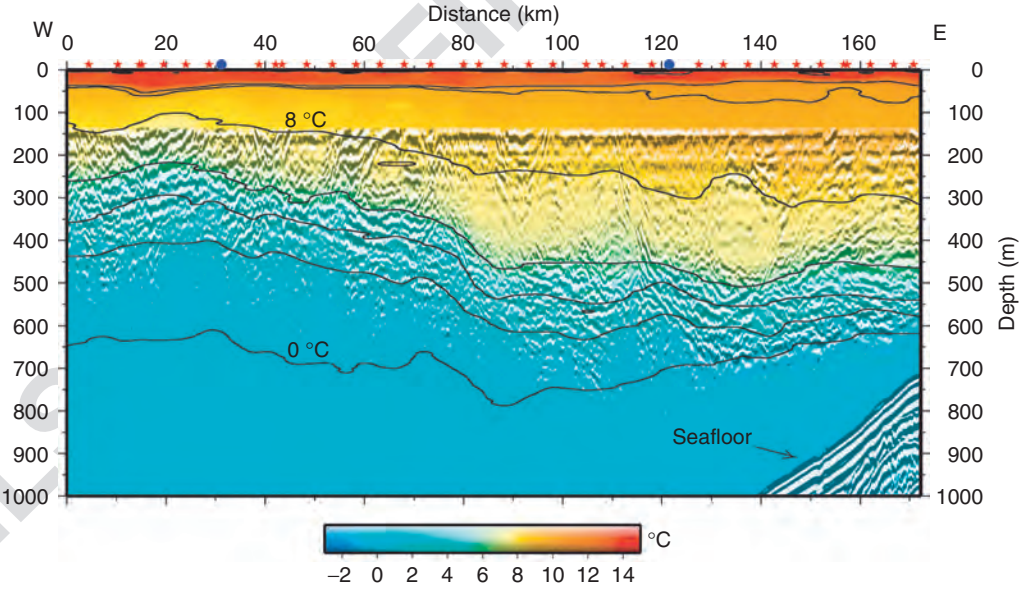

F0010 **Figure 2** Ocean temperature (color) overlain by seismic reflection data (black). Thin solid lines are selected isotherms contoured every 2 °C, derived from XBT and XCTD casts. Red stars and blue circles at top show locations of XBTs and XCTDs, respectively. The warm (7–14 °C) AW is separated from the cold (− 0.5–2 °C) NSDW by a boundary layer delineated by rapidly changing temperatures and strong seismic reflections. The top 140 m of the seismic profile, containing interference from the direct arrival, has been muted. From Nandi P, Holbrook WS, Pearse S, Páramo P, and Schmitt RW (2004) Seismic reflection imaging of water mass boundaries in the Norwegian Sea. *Geophysical Research Letters* 31: L23311 (doi:10.1029/ 2004GL021325). Copyright [2004] American Geophysical Union. Reproduced by permission of American Geophysical Union.

the front as a result of the geotrophic dynamical balance. Coherent slabs of 100- to 300-m-thick reflections inclined at 1–4° from the horizontal become progressively weaker and lose coherency with increasing depth, reaching down to about 1.5 s two-way-travel time (TWTT, approximately 1100 m depth).

P0045 Soon after the discovery of the ability to seismically image oceanic thermohaline fine-structure in such detail, the first joint seismic reflection/physical oceanography study was conducted in the Norwegian Sea: a dense array of expendable bathythermographs (XBTs) and expendable conductivity-temperature depth (XCTD) probes were deployed on several lines during the acquisition of seismic reflection data. The resulting data showed conclusively that the marine seismic reflection method can map distinct water masses. At the survey site, the major water masses are the warm and saline Atlantic Water (AW) carried by the Norwegian Atlantic current and underlying cold and less saline Norwegian Sea Deep Water (NSDW). Relatively nonreflective zones in the upper ~400 m and below the 0 °C isotherm in **Figure 2** correspond to AW and NSDW, respectively. Fine-scale temperature variability measured by the XBT/XCTDs in the boundary between the two water masses affects the sound speed and results in acoustic impedance contrasts manifested by the strong reflective zone in **Figure 2**.

P0050 Reflections generally follow isotherms derived from the XBT/XCTD survey (**Figure 2**). A comparison of a temperature profile measured by an XCTD to the coincident seismic reflection profile reveals the sensitivity of the reflections to fine-scale variability in temperature. Temperature fluctuations derived by high-pass filtering the temperature profile for lengths smaller than 35 m, the dominant wavelength of the range of the sound source used in this study, match the seismic reflection signal (**Figure 3**). Reflector amplitudes are enhanced where temperature anomalies are large. Even temperature fluctuations as small as 0.04 °C, comparable to the measurement accuracy of ±0.02 °C, can be imaged with seismic reflection techniques.

P0055 Seismic profiles across the Kuroshio current, off the Muroto peninsula southwest of Japan, revealed fine structure continuous at a horizontal scale over 40 km between 300 and 1000 m depth (**Figure 4**). Successive seismic profiles at 2–3 day intervals, corresponding to about cross-section snapshots every 180–450 km of the Kuroshio current moving with 1 m s^{-1}, suggest that the lateral continuity of the fine structure at the Kuroshio current is not a transient feature and can persist at least for 20 days.

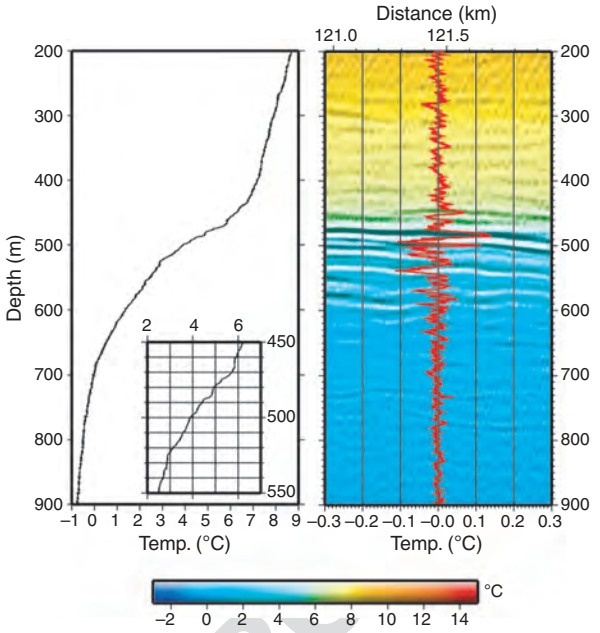

Figure 3 (a) An unfiltered XCTD profile located at km 121.5 on the seismic profile (**Figure 2**) showing temperature from 200–900 m depth. (b) Short-wavelength temperature variations (red), produced by removing wavelengths greater than 35 m from the XCTD temperature profile, plotted with a 5-km-wide section of the reflection image surrounding the XCTD location (black and white image). Background color scheme is ocean temperature, plotted as in **Figure 2**. The seismic image has been shifted upward by 14 m to reflect the lag between the onset of energy and peak amplitude in the seismic wavelet. From Nandi P, Holbrook WS, Pearse S, Páramo P, and Schmitt RW (2004) Seismic reflection imaging of water mass boundaries in the Norwegian Sea. *Geophysical Research Letters* 31: L23311 (doi:10.1029/2004GL021325). Copyright [2004] American Geophysical Union. Reproduced by permission of American Geophysical Union. F0015

P0060 The observations across the Kuroshio current motivated a joint seismic reflection and physical oceanographic survey in summer 2005 within the Kuroshio extension front east of Japan, where warm Kuroshio current meets cold Oyashio water. The hydrography and ocean currents were sampled using XBT, XCTD, expendable current profiler (XCP), and vessel-mounted acoustic Doppler current profiler (ADCP). Isotherms derived from XCTD measurements across the Kuroshio current show the temperature characteristics of the frontal system with intrusive features (**Figure 5(a)**). Two lines were acquired, one to the north (Line 1) and another to the south (Line 2) of the Kuroshio current core. The first-order difference in the seismic images is that the reflectors become nearly horizontal in Line 2 with increasing distance from the front, whereas more fine structure and steeply inclined reflectors are common in Line 1, consistent with the temperature section

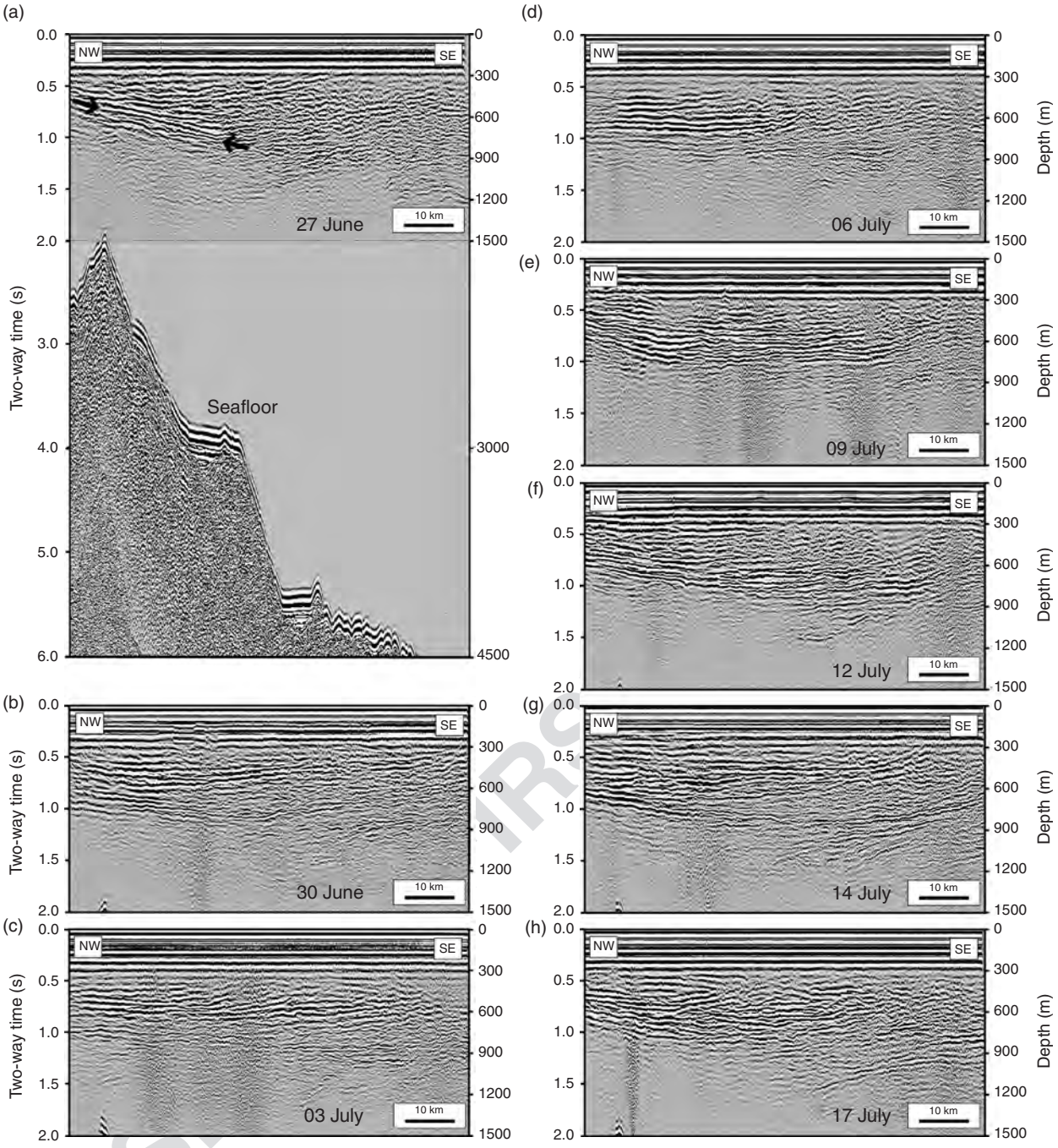

F0020 **Figure 4** Selected seismic profiles acquired across the Kuroshio current at 2–3 day intervals with date indicated on each panel. The orientation of the line is northwest (left) to southeast (right). The vertical axis to the left is the TWTT and that on the right is the depth calculated assuming an acoustic velocity of 1500 m s^{-1}. The image for (a) 27 June is shown for TWTT 0–6 s, whereas other panels are shown for 0–2 s. The reflection marked in (a) with arrows has a slope of ~1/120. From Tsuji T, Noguchi T, Niino H, *et al.* (2005) Two-dimensional mapping of fine structures in the Kuroshio Current using seismic reflection data. *Geophysical Research Letters* 32: L14609 (doi:10.1029/ 2005GL023095). Copyright [2005] American Geophysical Union. Reproduced by permission of American Geophysical Union.

(**Figure 5**(**a**)). With the purpose of determining the best seismic source configuration to image the oceanic fine structure, the seismic lines of this survey were repeated with different air gun chamber volumes (20 l, 9 l, and a 3.4 l air gun of generator–injector, GI, type). Upper portions of panels (b) to (c) of **Figure 5** show Line 1 sampled with decreasing air gun source strength over a duration of 54 hours. The

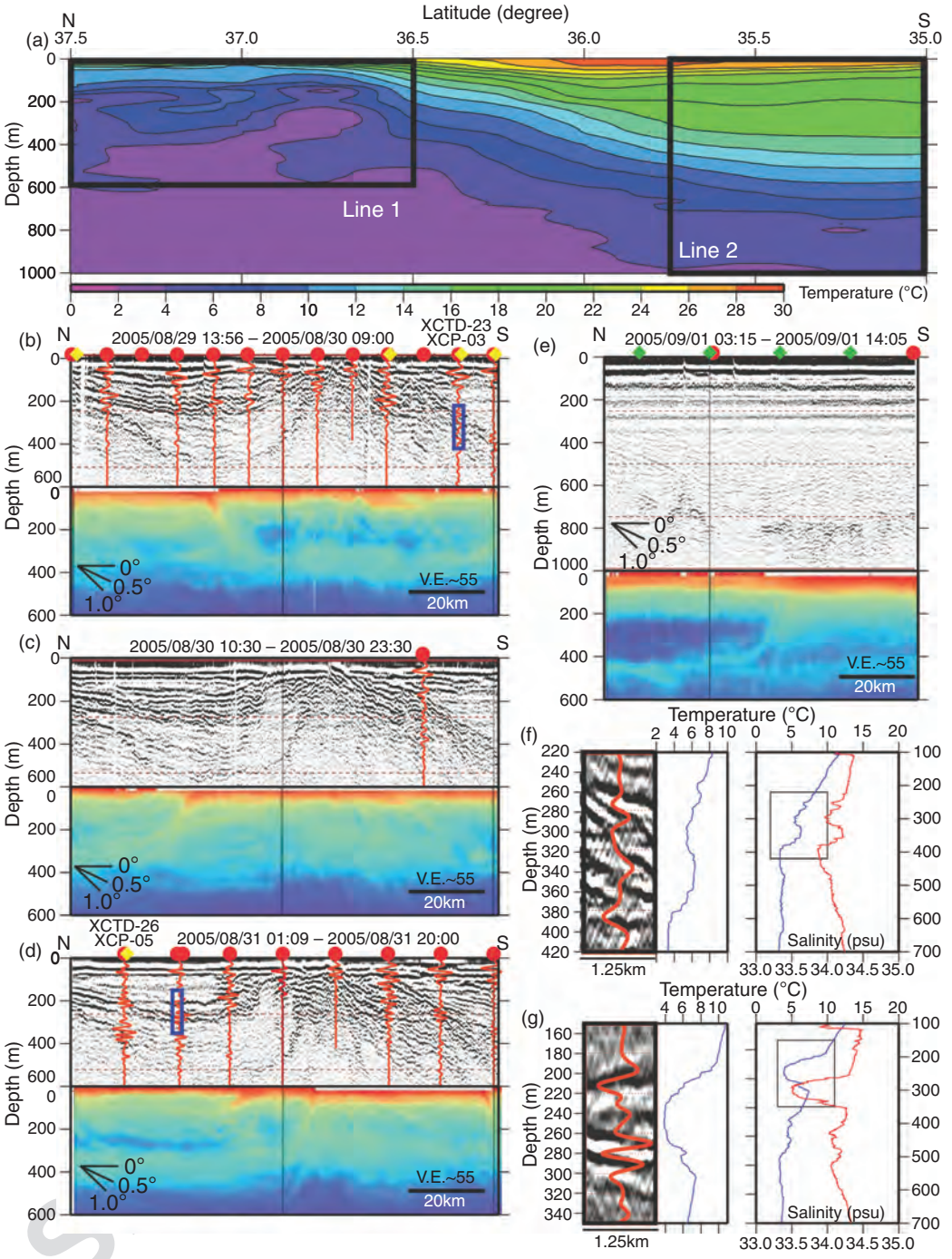

F0025 **Figure 5** Joint physical oceanography and marine seismic reflection survey within the Kuroshio extension front east of Japan. Two seismic lines, indicated by boxes in (a) were sampled: Line 1 to the north and Line 2 to the south of the core of the Kuroshio current. (a) Temperature section derived from XCTD measurements. Panels (b) to (e) show seismic reflection profile (gray scale, top) and ADCP intensity (color, bottom) for (b–d) Line 1 and (e) Line 2. The air guns used are (b) 20 l, (c) 9 l, (d) 3.4 l, and (e) 20 l. Time period of observation is indicated above each seismic profile. Red circles, green diamonds, and yellow diamonds are XCTD, XBT, and XCP locations, respectively. Red waveforms on the seismic reflection profiles are synthetic seismograms calculated from XCTD profiles. Expanded data from two blue rectangles marked in (b) and (d) are shown in (f) and (g), respectively. (f) Comparison of Line 1 seismic profile (20 l air gun) and XCTD data marked with blue rectangle in (b). (left) Seismic profile overlain by a synthetic seismogram (red), (right) temperature (blue) and salinity (red) profiles derived from XCTD measurements. (middle) Blow-up of temperature from the rectangle to the right, which corresponds to the depth range of seismic profile to the left. (g) Same as (f) except using 3.4 l air gun at location shown by blue rectangle in (d). From Nakamura Y, Noguchi T, Tsuji T, Itoh S, Niino H, and Matsuoka T (2006) Simultaneous seismic reflection and physical oceanographic observations of oceanic fine structure in the Kuroshio extension front. *Geophysical Research Letters* 33: L23605 (doi:10.1029/ 2006GL027437). Copyright [2006] American Geophysical Union. Reproduced by permission of American Geophysical Union.

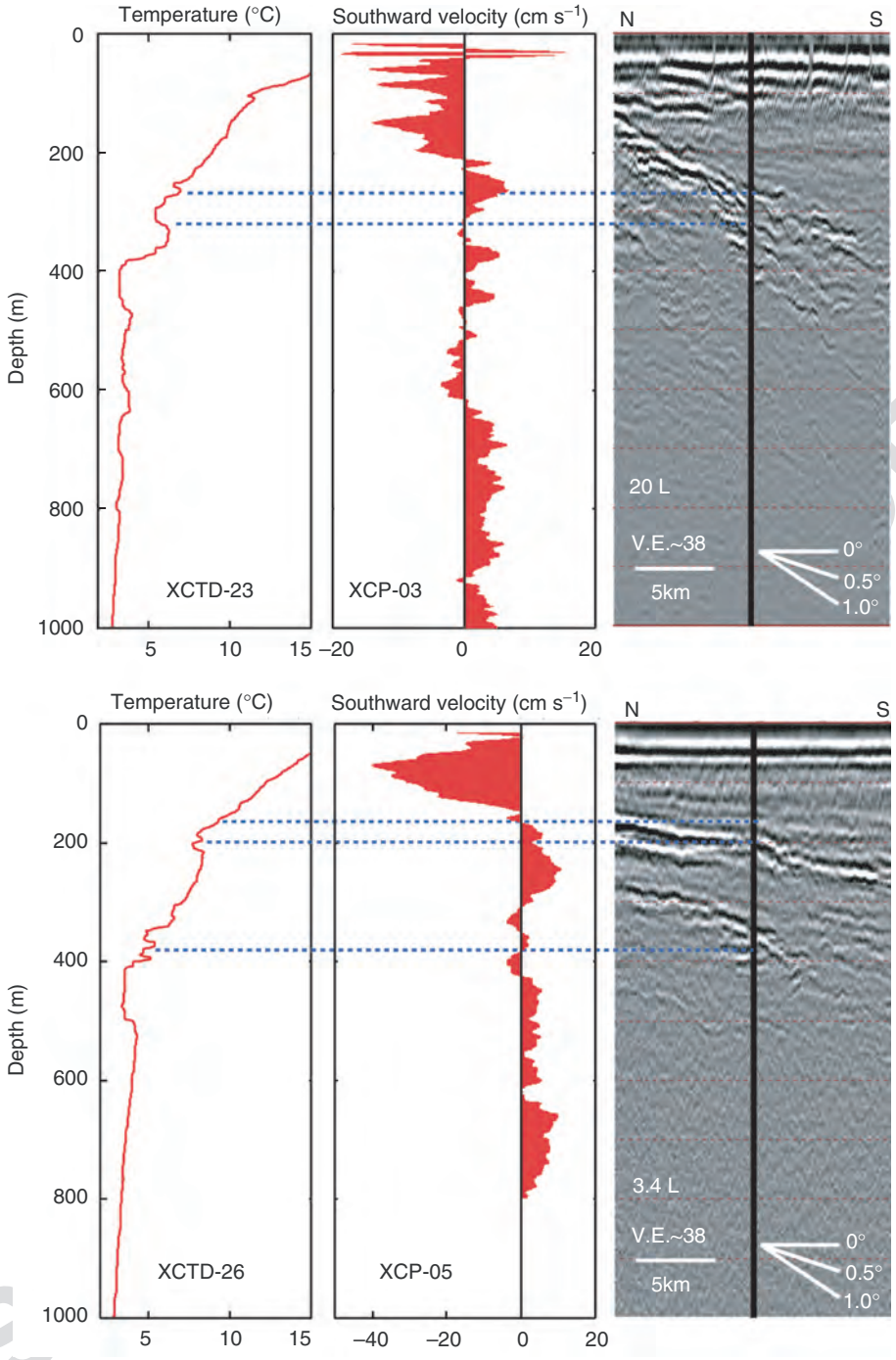

F0030 **Figure 6** Comparison of (left) XCTD temperature, (middle) southward velocity recorded by XCP and (right) seismic reflection data. XCTD and XCP station numbers indicated on panels are marked in **Figure 5(b)** and **5(d)**. The dashed blue horizontal lines indicate abrupt temperature and velocity changes correlated with seismic reflections. Location of the XCP and XCTD measurements relative to the seismic profile is shown by vertical black lines. All data are collected at Line 1 (see **Figure 5a**) with top panels using a 20 l air gun and bottom panels using a 3.4 l air gun. These two measurements were separated in time by ~19 hours. From Nakamura Y, Noguchi T, Tsuji T, Itoh S, Niino H, and Matsuoka T (2006) Simultaneous seismic reflection and physical oceanographic observations of oceanic fine structure in the Kuroshio extension front. *Geophysical Research Letters* 33: L23605 (doi:10.1029/ 2006GL027437). Copyright [2006] American Geophysical Union. Reproduced by permission of American Geophysical Union.

reflection patterns are consistent between consequent transects and correlate with hydrographic property changes in the water column. Depth-distance maps of the ADCP backscatter intensity collected in concert with the seismic reflection data show some similarities to the seismic images regarding the inclined reflection patterns and their locations. Similar to the observations in the Norwegian Sea (**Figure 2**) reflections are enhanced at the base of the thermocline (temperature range 4–8 °C).

P0065 Given an observed CTD profile a synthetic reflection pattern can be constructed to check whether the seismic interpretation of thermohaline fine structure is credible or not. The sound speed profile in seawater (calculated as a function of temperature, salinity and depth) is used to calculate acoustic impedance contrasts. Acoustic impedance is relatively more sensitive to changes in sound speed than changes in density. Reflection coefficients derived from acoustic impedance are used to generate synthetic seismograms. Red waveforms on the seismic reflection profiles of **Figure 5** are such synthetic seismograms constructed from the XCTD profiles. The synthetic profiles match the seismic observations well, lending confidence to the physical interpretation of the reflectors (**Figure 6**). AU1

P0070 Common in all seismic reflection images are undulations of reflectors which cannot be attributed to

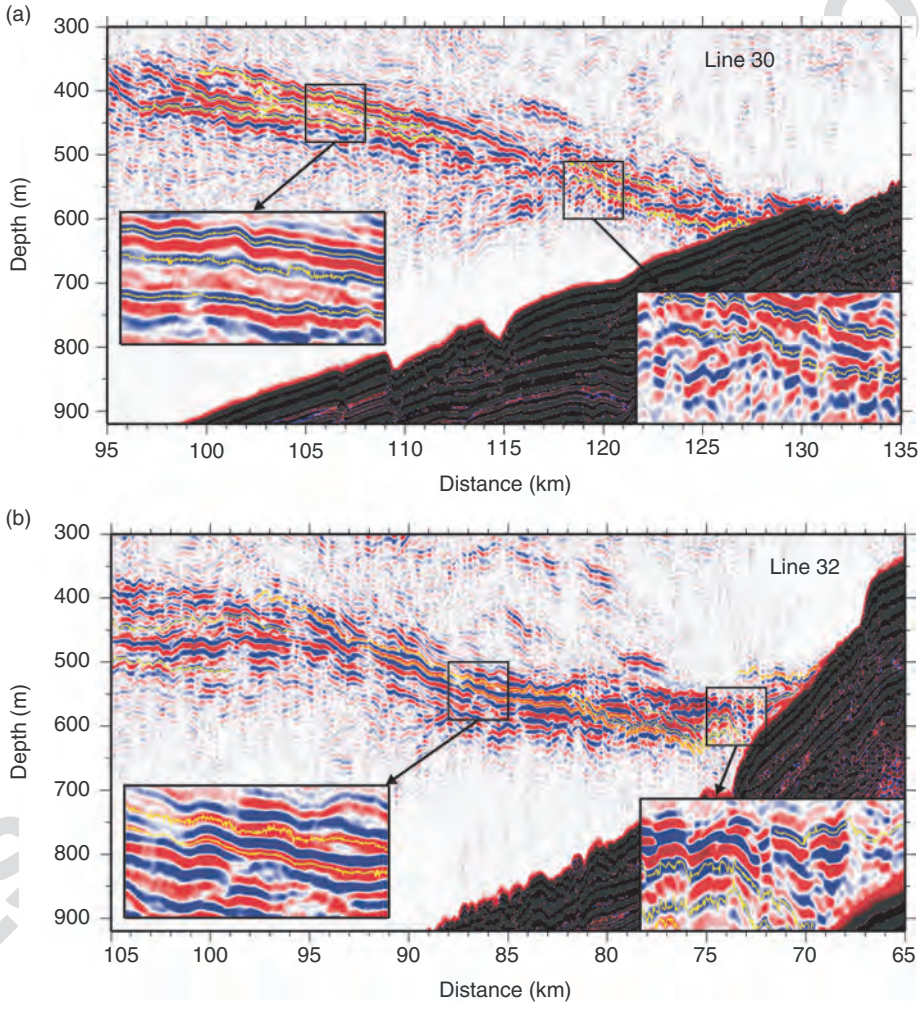

F0035 **Figure 7** Seismic sections for Lines (a) 30 and (b) 32 acquired across the isobaths in the Norwegian Sea. Data are displayed so that peaks and troughs of reflections are red and blue, respectively, in the water column, and grey and black in the solid earth. Yellow lines show reflectors picked and digitized by auto-tracking for spectral analysis shown in **Figure 8**. (a) Stacked seismic section of line 30 shows a clear progression toward the slope from smooth, continuous fine structure (inset left) to highly disrupted fine structure (inset right). (b) Stacked seismic section of Line 32, similar to Line 30, shows fine structure changing from smoothly undulating to more discontinuous pattern as the continental slope is approached. From Holbrook WS and Fer I (2005) Ocean internal wave spectra inferred from seismic reflection transects. *Geophysical Research Letters* 32: L15604 (doi:10.1029/ 2005GL023733). Copyright [2005] American Geophysical Union. Reproduced by permission of American Geophysical Union.

processing artifacts. It is well known that the velocity shear of the internal wave field of the stratified ocean displaces the isopycnals, isotherms, and irreversible fine structure caused by mixing events. The undulating reflectors can be interpreted as the acoustic snapshots of the fine structure displacements due to the internal waves. This assertion was recently tested by digitizing selected reflectors where reflectors roughly parallel isotherms (hence representative of isotherm displacements) and comparing the wavenumber spectrum to the isopycnal displacement expected from oceanic internal wave field. In the open ocean, frequency and wavenumber domain representations of internal wave energy show a remarkably uniform energy spectrum that can be modeled by the so-called Garrett–Munk spectrum, which has a frequency, ω, and wavenumber, k, decay of energy with a power law near ω^{-2} and k^{-2}. This spectrum is thought to be maintained by a cascade of energy from large scales and low frequencies to small scales and high frequencies due to interaction of different wave packets. Two seismic lines presented in **Figure 7** were acquired in the Norwegian Sea at 6.25 m horizontal resolution. Reflectors roughly following the isotherms derived from XBT measurements in the vicinity are digitized (yellow traces in **Figure 7**) to calculate the horizontal wavenumber (k_x) power spectra of reflection displacements, ζ, obtained by removing a straight line fit over the extent of each reflector (typically 5–30 km).

P0075 It is known that the internal wave characteristics differ significantly in proximity to the sloping boundaries where internal wave–boundary interactions lead to a variety of processes that can enhance the internal wave energy, shear, and mixing. Consistently, the seismic reflection images show a marked change from smooth, continuous patterns to more choppy reflections with high vertical displacements as the continental slope is approached. The spectra calculated away from the seafloor and horizontally within 10 km of the continental slope are compared to the Garrett–Munk spectrum in **Figure 8**. For the open ocean reflectors, the agreement with the oceanic internal wave horizontal wave number spectrum is within a factor of 2 down to wavelengths of about 30 m. Near the continental slope reflector displacement spectrum suggests enhanced internal wave energy which could be caused by wave reflection and generation processes at the sloping boundary. At a length scale of about 300 m, there is an apparent change of slope from k_x^{-2} of the internal wave spectrum to $k_x^{-5/3}$ of the inertial subrange of turbulence. Consistent with this inference from the seismic profiles, recent measurements of joint isopycnal displacement and turbulence dissipation rates indicate that turbulence subrange extends to surprisingly large horizontal wavelengths

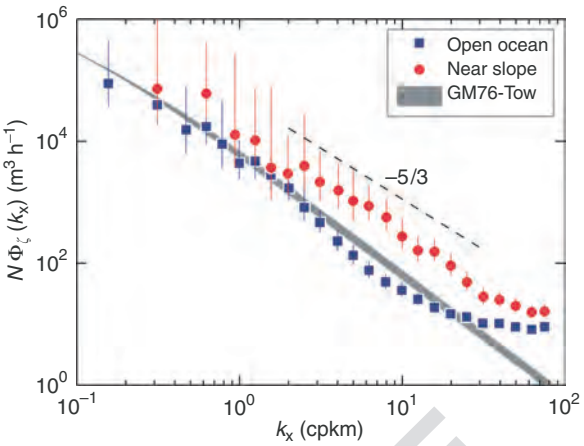

Figure 8 Horizontal wavenumber spectra of vertical displacements inferred from digitized reflectors from open ocean (squares), near slope (dots), all scaled by the average buoyancy frequency, N, covering the representative depth range of the chosen reflectors. Vertical bars are 95% confidence intervals. Garrett–Munk tow spectrum is shown as a band for the observed range of $N = (1.7 - 4.4) \times 10^{-3}\,s^{-1}$. The dashed line shows the −5/3 slope of the inertial subrange of turbulence, for reference. From Holbrook WS and Fer I (2005) Ocean internal wave spectra inferred from seismic reflection transects. *Geophysical Research Letters* 32: L15604 (doi:10.1029/2005GL023733). Copyright [2005] American Geophysical Union. Reproduced by permission of American Geophysical Union. F0040

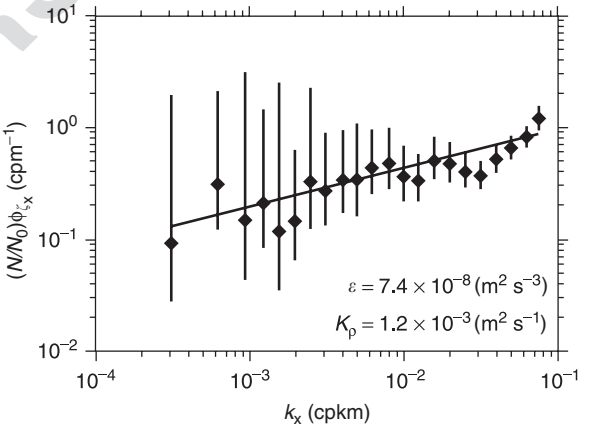

Figure 9 Reflection-slope spectrum, $\phi_{\zeta x}$, derived from the near-slope spectrum shown in **Figure 8**. Spectrum is normalized by the buoyancy frequency, $N = 3.5 \times 10^{-3}\,s^{-1}$, relative to $N_0 = 5.3 \times 10^{-3}\,s^{-1}$. Dissipation rate of turbulent kinetic energy, ε, is estimated by a fit of the turbulent spectrum in the $4 \times 10^{-3} - 2 \times 10^{-2}$ cpm wavenumber range. Eddy diffusivity is estimated using $K_\rho = 0.2\varepsilon/N^2$. Reproduced with permission from Klymak JM and Moum JN (2007) Oceanic isopycnal slope spectra: Part II: Turbulence. *Journal of Physical Oceanography* 37: 1232–1245. F0045

(>100 m). A fit of the spectral amplitude to a turbulence model spectrum yields reasonable estimates of the turbulent dissipation rate in the water column, even when applied to horizontal scales of tens of meters, which could not be possible in vertical profiles. The method is equally applicable to horizontal transects of seismic reflectors which follow isopycnal displacements. A fit to the near-slope spectrum of **Figure 8** predicts diapycnal eddy diffusivity on the order $\sim 10^{-3}\,m^2\,s^{-1}$ (**Figure 9**).

S0025 ## Conclusions

P0080 Standard multichannel marine seismic reflection profiling has the capability to image order 10 m vertical scale sound speed and density fine structure in the ocean, if processing gains are sufficiently high. Seismic reflection images visualize ocean fronts, water mass boundaries, eddies, intrathermocline lenses, and thermohaline intrusions. With the very dense lateral sampling of reflection profiling (order 10 m), exceptional detail can be seen in the structure of oceanic reflectors throughout portions of the water column where fine structure is present. Interpreting marine seismic reflection data in terms of ocean fine structure and internal motions is presently being investigated to develop this technique into a tool that can produce useful and trusted information on properties of dynamical interest to the physical oceanographers. A basic physical understanding is achieved on the origin of low-frequency reflections in the water column. Carefully analyzed horizontal transects of reflectors suggest that undulating patterns common in most seismic transects are a proxy to the isopycnal displacements and can be used to remotely estimate the internal wave energy as well as turbulent kinetic energy dissipation rate and mixing where ocean fine structure allows. In the near future, joint seismic-physical oceanography surveys are anticipated, which will provide ground-truth and further improvements in interpreting and analyzing seismic reflection sections and finally allow for exploitation of the extensive global archive of marine seismic reflection data for interpreting the ocean dynamics.

Nomenclature

k	wavenumber (cycles per meter, cpm)
k_x	horizontal wavenumber (cycles per meter, cpm; or cycles per kilometer, cpkm)
K_ρ	Diapycnal eddy diffusivity ($m^2\,s^{-1}$)
N	Buoyancy frequency (s^{-1})
ε	Dissipation of turbulent kinetic energy, per unit mass ($m^2\,s^{-3}$)
ζ	vertical displacement (m)
ζ_x	horizontal derivative of ζ (–)
ω	Frequency (Hz)

See also

Acoustics, Deep Ocean (00312). Double-diffusive Convection (00604). Internal Waves (00126). Kuroshio and Oyashio Currents (00350). Sonar Systems (00317).

Further Reading

Holbrook WS and Fer I (2005) Ocean internal wave spectra inferred from seismic reflection transects. *Geophysical Research Letters* 32: L15604 (doi:10.1029/ 2005GL023733).

Holbrook WS, Páramo P, Pearse S, and Schmitt RW (2003) Thermohaline fine structure in an oceanographic front from seismic reflection profiling. *Science* 301: 821–824.

Klymak JM and Moum JN (2007) Oceanic isopycnal slope spectra: Part II: Turbulence. *Journal of Physical Oceanography* 37: 1232–1245.

Nakamura Y, Noguchi T, Tsuji T, Itoh S, Niino H, and Matsuoka T (2006) Simultaneous seismic reflection and physical oceanographic observations of oceanic fine structure in the Kuroshio extension front. *Geophysical Research Letters* 33: L23605 (doi:10.1029/ 2006GL027437).

Nandi P, Holbrook WS, Pearse S, Páramo P, and Schmitt RW (2004) Seismic reflection imaging of water mass boundaries in the Norwegian Sea. *Geophysical Research Letters* 31: L23311 (doi:10.1029/ 2004GL021325).

Páramo P and Holbrook WS (2005) Temperature contrasts in the water column inferred from amplitude-versus-offset analysis of acoustic reflections. *Geophysical Research Letters* 32: L24611 (doi:10.1029/ 2005GL024533).

Tsuji T, Noguchi T, Niino H, *et al.* (2005) Two-dimensional mapping of fine structures in the Kuroshio current using seismic reflection data. *Geophysical Research Letters* 32: L14609 (doi:10.1029/ 2005GL023095).

Biographies

Ilker Fer (Ph.D. 2001) is associate professor of physical oceanography at the Geophysical Institute, University of Bergen. Fer is also affiliated with the Bjerknes Centre for Climate Research in Bergen. He has had over 10 years of field experience at sea and in lakes with focus on small scale processes, turbulence and mixing, including work from icebreakers and drifting ice camps. His research interests cover dense water overflows, turbulence, fine and microstructure data acquisition and interpretation, newly-developing seismic reflection techniques to image oceanic finestructure, convective processes leading to dense water formation, turbulence in the under ice boundary layer, air-ice-sea interaction, internal waves and their non-linear interaction and turbulence parameterizations.

W. Steven Holbrook (Ph.D. 1989) is professor of geophysics at the University of Wyoming. Holbrook is also adjunct scientist at the Woods Hole Oceanographic Institution since 2004. He has over 20 years of field experience on seismic and geological studies. His group in Wyoming has recently made the exciting discovery of imaging of the ocean thermohaline structure using seismic reflection profiling techniques. His present research focuses on several aspects of oceanography, including imaging eddies, water mass boundaries and thermohaline staircases, and cataloging internal wave spectra through seismic reflection measurements.